31st Congress of the International Council of the Aeronautical Sciences
Belo Horizonte, Brazil; September 09-14, 2018

COUPLED ADJOINT AEROSTRUCTURAL OPTIMIZATION FRAMEWORK FOR PRELIMINARY AIRCRAFT DESIGN

Charles M. Boozer *, Ali Elham *
***Technische Universität Braunschweig**
Keywords: *MDO, Coupled Adjoint, Aerostructural Optimization, Aircraft Design*

Abstract

In order to explore and exploit the full potential of aircraft design, the aircraft must be designed as it is, a coupled system. Previous works have laid the foundation for this path by developing a tool for wing aerostructural optimization. In this work, the tool is extended to include the horizontal stabilizer. An aeroelastic optimization is performed to validate the methods used to estimate weight and sensitivities, while an aerostructural optimization is performed to exhibit the performance of the tool in its current state. The aerostructural optimization shows both improvements in the configuration, such as an 8.2% reduction in fuel weight, while also exhibiting the additional complexities and requirements for the optimization framework when considering more than just the wing in the aircraft system.

1 Introduction

Sustainability and fuel efficiency are the main design drivers of the next generation of the passenger aircraft. As a result, the Advisory Council for Aviation Research and Innovation in Europe defined the goal of the design of passenger aircraft for the year 2050 to be 75% reduction in CO_2 emission, 90% reduction in NO_x and 65% reduction in noise compared to the year of 2000 [1]. To achieve such a goal the traditional, i.e. statistical and empirical based, design methodologies need to be replaced by the advanced Multidisciplinary Design optimization (MDO) based design methodologies.

Aerodynamics and structure are the main disciplines in aircraft design using the MDO techniques. Applications of the high fidelity aerostructural optimizations to the design of aircraft lifting surfaces can be found in literature. The main drawback of high fidelity optimization is the enormous required computational power. Executing such MDO tasks needs massive parallel computing, which mean high computational cost. During early design steps, where a wide range of design variables need to be optimized, paying such a high price for MDO may not be feasible.

The goal of this research is to develop an aerostructural analysis and optimization method/tool for aircraft preliminary design, where the computational cost is much lower than the high-fidelity optimization methods, but the same level of accuracy is still quite comparable. Previous steps in this research have produced such a tool for aircraft wings, but in this step, that tool is extended with the inclusion of the horizontal stabilizer.

2 Coupled Multidisciplinary Analysis

The immediate obstacle in aeroelastic and aerostructural optimizations is to solve the coupled problem containing the structural, aerodynamics, and performance disciplines. For this the Finite-element-based Elham Modified Weight Estimation Technique (FEMWET) is used. Detailed information regarding the existing wing analysis and optimization features of FEMWET can be found in [2, 3], while new features regarding the addition of the horizontal tail are included in this work.

2.1 Structural Analysis

The structural analysis is based on a finite element beam model utilizing consistent, 3D, 2-

node Timoshenko beam shape functions where the cross section is represented by the wingbox. Solving the structural governing equation

$$KU = F \tag{1}$$

where K is the element stiffness matrix and F is the force vector provides U, the nodal displacement vector. Once the displacements are obtained the stress distribution among the wingbox equivalent panels can be determined. Finally, these stresses along with the structure's material properties are used to evaluate yield and buckling failure criteria.

The equivalent panels' thicknesses must be such that the structure does not fail under any of the load conditions. Once these thicknesses are determined, the structural weight of the lifting surface can be determined. Two empirical equations are used to determine the weight of the wing and horizontal stabilizer respectively. The two equations are

$$W_w = 1.5W^{F.E.}_{wingbox,w} + 15S_w \tag{2a}$$
$$W_h = 1.5W^{F.E.}_{wingbox,h} + 10S_h \tag{2b}$$

where W is the weight of the surface, $W^{F.E.}_{wingbox}$ is the weight of the finite element wingbox, S is the reference area, and the subscripts w and h denote values for the wing and horizontal respectively. The first factor, 1.5, accounts for the weights that are not modeled. The second factor, 15 for the wing and 10 for the horizontal, represents the secondary weights such as the leading and trailing edges, flaps, slats, etc.

2.2 Aerodynamic Analysis

The aerodynamic component of the FEMWET tool utilizes a quasi-three-dimensional (Q3D), method which combines a vortex lattice method (VLM) code based on the methods presented by Katz and Plotkin [4] and the two-dimensional, compressible airfoil analysis tool MSES [5]. The VLM code is governed by the following equation

$$AIC\,\Gamma = V \tag{3}$$

where AIC is the aerodynamic influence matrix, Γ is the vortex strengths, and V is the right-hand side. AIC and V are determined by the geometrical layout of the vortex panels, thus once Γ is obtained the loading and induced drag of the surfaces can be calculated. At high Mach numbers the Prandtl-Glauert compressibility correction is used. MSES is coupled to the VLM results by matching the lift coefficients obtained at different spanwise stations. The governing equation for this coupling is

$$c_{l,\ VLM} = c_{l,\ MSES} \tag{4}$$

where c_l is the section lift coefficient calculated using VLM and MSES respectively. The two values are coupled using an incidence angle state variable, α_i. Once matched, MSES calculates the pressure, viscous, and wave drag for each airfoil section.

An important constraint to include in the aeroelastic and aerostructural optimizations is aileron effectiveness. Defined as the ratio of the roll moment due to aileron deflection for an elastic case to a rigid case:

$$\eta_a = \frac{C_{l_{\delta\,elastic}}}{C_{l_{\delta\,rigid}}} \tag{5}$$

aileron effectiveness is used as a metric to constrain the wing's torsional stiffness. In Eq. (5) C_l is the rolling moment for the elastic and rigid wings respectively. This constraint helps eliminate the possibility of aileron reversal during the optimizer's attempt to reduce structural weight.

Two governing equations remain and are shown below:

$$L = nW_{case} \tag{6}$$
$$C_{m,\ C.G.} = 0 \tag{7}$$

The first equation, where L is the lift of the aircraft and W_{case} and n are the weight of the aircraft and load factor for the specific load case respectively, requires the lift of the full aircraft to equal the weight of the aircraft for the specific load case. The lift and weight coupling is controlled by the state variable α, or angle of attack.

The second equation is a new addition to the FEMWET software due to the addition of the horizontal stabilizer and determines its incidence angle, i_{ht}. Eq. (7) states there should be no residual pitching moment about the center of gravity of the aircraft, or that the aircraft is trimmed. The pitching moment coefficient is calculated using the expression below:

$$C_{m,\ C.G.} = \left(-L_w\left(x_{AC,w} - x_{C.G.}\right) - L_h\left(x_{AC,h} - x_{C.G.}\right)\right) / (q S_w \bar{c}) \tag{8}$$

In Eq. (8) L is the lift force on the surface, x_{AC} is the location of the aerodynamic center, $x_{C.G.}$ is the location of the center of gravity, q is the dynamic pressure, and $\bar{c}$ is the mean aerodynamic chord of the wing.

2.3 Aero-structural Coupling

The coupled physics problem, governed by Eqs. (1, 3-4, 6-7), must be solved in an efficient manner, as a solution is required for each optimization iteration. There are five state variables shared between the five governing equations: Γ, U, α, α_i, and i_{ht}. The coupled system can be written as shown below:

$$\begin{bmatrix} A(X,\Gamma,U,\alpha,i_{ht}) \\ S(X,\Gamma,U) \\ W(X,\Gamma) \\ C(X,\Gamma,U,\alpha,a_i,i_{ht}) \\ M(X,\Gamma) \end{bmatrix} = \begin{bmatrix} AIC\,\Gamma - V \\ KU - F \\ L - W_{des}n \\ c_{l,\ VLM} - c_{l,\ MSES} \\ C_{m,\ C.G.} \end{bmatrix} = 0 \tag{9}$$

In Eq. (9) X is the design vector, discussed in the optimization section. In Eq. (3), AIC and V are functions of the displacement vector U. V is also a function of α and i_{ht}, which determine the angle at which the flow encounters the surfaces. The force vector in Eq. (1) and lift in Eq. (6) are functions of Γ. In Eq. (4), $c_{l,\ VLM}$ is a function of Γ and $c_{l,\ MSES}$ is a function of all other state variables. In addition, all of the governing equations are functions of the design vector.

The Newton method is used to solve the coupled system and provides two advantages to the optimization routine. First, a consistent solution is obtained and second, derivatives used to converge the solution can be provided to the optimization algorithm, discussed later, to reduce the computational effort. During the Newton iterations, X remains constant and the solution is converged by stepping each of the state variables to convergence to provide a consistent solution. The new step, or update vector, can be calculated by solving the system of equations below:

$$\begin{bmatrix} \partial A/\partial Y \\ \partial S/\partial Y \\ \partial W/\partial Y \\ \partial C/\partial Y \\ \partial M/\partial Y \end{bmatrix} \begin{bmatrix} \Delta\Gamma \\ \Delta U \\ \Delta\alpha \\ \Delta a_i \\ \Delta i_{ht} \end{bmatrix} = - \begin{bmatrix} A(X,\Gamma,U,\alpha,i_{ht}) \\ S(X,\Gamma,U) \\ W(X,\Gamma) \\ C(X,\Gamma,U,\alpha,a_i,i_{ht}) \\ M(X,\Gamma) \end{bmatrix} \tag{10}$$

where $Y = [\Gamma, U, \alpha, a_i, i_{ht}]$

Eq. (10) can also be written as

$$\partial R/\partial Y\ \Delta Y = -R \tag{11}$$

where $\partial R/\partial Y$ is a square matrix containing derivatives in the arrangement of $\partial R_i/\partial Y_j$.

2.4 Sensitivity Analysis

Gradient-based optimization methods typically have one major drawback for complex problems, the computation of the derivatives. The total derivatives can be the most difficult, especially when utilizing existing software packages and solving coupled problems. One method, coupled adjoint sensitivity analysis, can greatly alleviate some of the problems by eliminating the total derivatives necessary to calculate the total derivative of the objective function with respect to the design vector, dJ/dX. However, the adjoint problem must be derived for the specific problem under consideration.

A detailed derivation of an aerostructural wing optimization problem using the coupled adjoint method can be found in [2]. A condensed derivation is shown here for brevity. First, the sensitivity of the objective function is expressed as:

$$\frac{dJ}{dX} = \frac{\partial J}{\partial X} + \frac{\partial J}{\partial Y}\frac{dY}{dX} \tag{12}$$

Taking the derivative of the residuals in Eq. (9) provides the following equation which can be solved for dY/dX.

$$\frac{dR}{dX} = \frac{\partial R}{\partial X} + \frac{\partial R}{\partial Y}\frac{dY}{dX} = 0 \quad (13a)$$

where $$\frac{dY}{dX} = -\frac{\partial R}{\partial Y}^{-1}\frac{\partial R}{\partial X} \quad (13b)$$

Substituting Eq. (13b) into Eq. (12) gives

$$\frac{dJ}{dX} = \frac{\partial J}{\partial X} - \Psi\frac{\partial R}{\partial X} \quad (14a)$$

where $$\Psi = \frac{\partial J}{\partial Y}\frac{\partial R}{\partial Y}^{-1} \quad (14b)$$

where Ψ is the gradient adjoint vector. From Eq. (14), we see that not only are the total derivatives eliminated, but $\partial R/\partial Y$ is already available due to the Newton iteration loop.

The various partial derivatives are calculated using analytical derivations, automatic differentiation, and the MSES software. Automatic differentiation is performed using the Matlab toolbox INTLAB [6]. MSES provides derivatives of the 2D lift and drag coefficients and utilizes the coupled adjoint method.

2.5 Validation

Both the structural and aerodynamic modules of FEMWET for wing analysis and design have been tested and validated, shown in [2] and [3] respectively. The structural weights of the wing and horizontal tail were validated in this work using an aeroelastic structural weight minimization, discussed in the next section, of the A320-200. The reference weights of each surface obtained from Obert [7] and the results of the optimization are recorded in Table 1. As shown, the weights closely match the reference values for the A320-200 with less than 1% error.

Table 1. Weight validation.

	Reference	FEMWET	Error
Wing	8801 kg	8861 kg	0.68%
Horizontal	625 kg	619 kg	0.96%

The sensitivities must also be validated. The following plots show derivatives of the new state

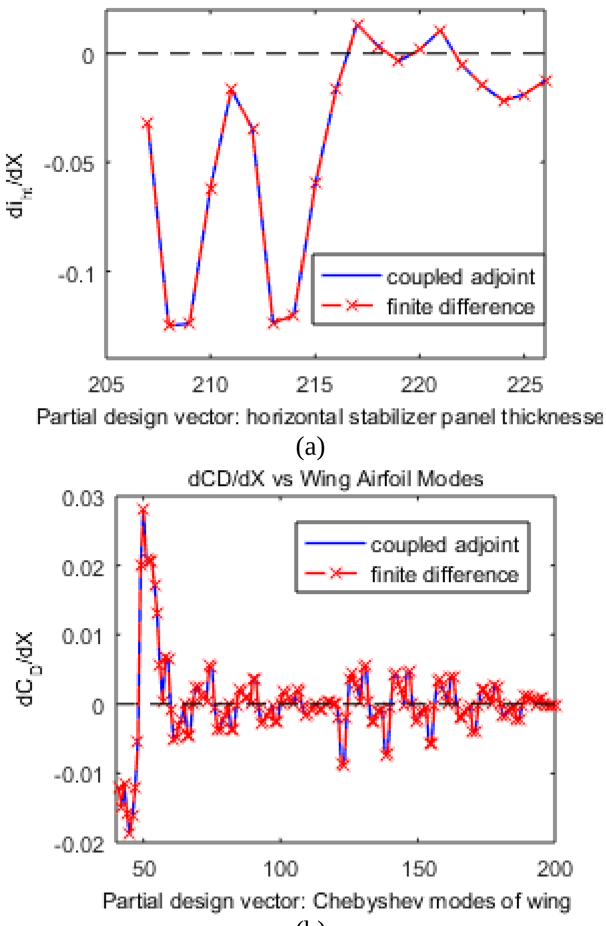

Fig. 1. (a) derivatives of i_{ht} with respect to the horizontal stabilizer panel thicknesses, (b) sensitivity of C_D with respect to the Chebyshev modes of the wing.

variable, i_{ht}, and the drag coefficient, C_D, both with respect to portions of the design vector. With the step length of $1\cdot10^{-6}$ used for the finite difference calculation, Figure 1 shows that the gradients from the coupled adjoint method agree with those from finite difference.

3 MDO Problem Definition

In this section the core components of the optimization problem are described: objective function, constraints, design vector, and sensitivities. In this work two problems are solved: aeroelastic optimization and aerostructural optimization. The aeroelastic optimization is solved first and used to obtain initial values of the structure variables, discussed later, such that the initial structure for the aerostructural problem is feasible.

3.1 Shape Parameterization

Manipulating the geometry and structure of a lifting surface requires efficient shape parameterization techniques. The first set of variables control the planform shape of the lifting surface. Variables include: root chord length, taper ratio, half-span length, sweep angle, root twist, and tip twist. Chebyshev mode shapes comprise the second set of design variables and are used to control the airfoil shapes of the surface.

Finally, the structure is modeled as the wingbox and includes a specified number of spanwise sections, each containing equivalent panels for the upper, lower, front, and rear corresponding to the upper and lower skins and front and rear spars respectively. The shape of the wingbox is determined by the first two sets of design variables, while the thicknesses of these panels are used as the last set of independent variables. The planform (*P*), mode shape (*G*), and thickness (*T*) vectors are assigned for each separate surface, such as wing and horizontal stabilizer and comprise the design vector.

3.2 Aeroelastic Optimization Problem

The objective for aeroelastic optimization is to minimize the structural weight of the lifting surfaces while ensuring the structure sustains the defined load cases. For this problem all aircraft parameters remain constant except for the structural variables. The optimization problem is written as:

$$\begin{aligned} \text{min} \quad & J(T) = \Sigma W_{surf}(T) \\ \text{w.r.t.} \quad & T \\ \text{such that:} \quad & Failure_k \leq 0 \\ & \frac{\eta_{a0}}{\eta_a} - 1 \leq 0 \\ & T_{lower} \leq T \leq T_{upper} \end{aligned} \tag{15}$$

Here W_{surf} is the weight of the lifting surface or surfaces included in the optimization problem, $Failure_k$ is the failure mode of the panels for each k-th load case, η_{a0} and η_a are the original and optimized aileron effectiveness respectively, and T_{lower} and T_{upper} are the upper and lower bounds for the panel thicknesses respectively. Details regarding the structural failure constraints is described in [2]. The surfaces may include either the wing, horizontal stabilizer, or both. The lower bound for *T* was defined using [8].

3.3 Aerostructural Optimization Problem

The objective for aerostructural optimization is to minimize the aircraft's fuel weight represented by the equation

$$W_F = 1.05\left(1 - M_{ff}\right) MTOW \tag{16}$$

where M_{ff} is the mass fuel fraction and *MTOW* is the maximum take-off weight. For the cruise segment of the mission, M_{ff} is computed using the Breguet range equation. For all other mission segments M_{ff} is computed using the method presented by Roskam [9]. The factor 1.05 accounts for 5% of the total fuel weight as reserve fuel. The design vector now includes the parameters *T*, *G*, and *P*, as well as two additional surrogate variables for the fuel weight and maximum take-off weight. The aerostructural optimization problem is written as:

$$\begin{aligned} \text{min} \quad & J(X) = W_F(X) \\ \text{w.r.t.} \quad & X = [T, G, P, W_{FS}, MTOW_S] \\ \text{such that:} \quad & Failure_k \leq 0 \\ & \frac{\eta_{a0}}{\eta_a} - 1 \leq 0 \\ & \frac{MTOW/S_w}{(MTOW/S_w)_0} - 1 \leq 0 \\ & \frac{W_F}{W_{FA}} - 1 \leq 0 \\ & \frac{W_F}{W_{FS}} - 1 = 0 \\ & \frac{MTOW}{MTOW_S} - 1 = 0 \\ & X_{lower} \leq X \leq X_{upper} \end{aligned} \tag{17}$$

Four new constraints appear in the aerostructural problem. The first new constraint shown in Eq. (17) is to keep the wing loading, defined as the maximum take-off weight divided by the wing reference area, less than or equal to the wing loading of the initial wing. This constraint is required to make sure the aircraft can satisfy the take-off and landing requirements. The last inequality constraint is for fuel volume and states that the fuel weight must be less than the available fuel weight. The two equality constraints state that the calculated value and surrogate value in the design vector, with subscript *s*, should be equivalent.

3.4 Optimization Architecture

Although minimizing two different objective functions subject to different constraints, the architecture for solving the optimization problems is identical. The multidisciplinary feasible (MDF) gradient-based optimization strategy [10] is used and is characterized by several key traits: the problem being optimized is coupled, a consistent solution is obtained at each optimization iteration, and the optimization may take longer to converge. As mentioned previously, the Newton iteration inside FEMWET provides the consistent solution to the optimizer. For all optimizations, the SNOPT optimization algorithm [11] was used as the optimizer.

4 Case Study

4.1 Problem Setup

The aircraft used in this work is the Airbus A320-200. The planform dimensions of the wing and horizontal stabilizer are shown in Figure 2. In Figure 2, c and b represent the chord and span length respectively. The horizontal stabilizer is modeled as one surface which moves as a whole, rather than a separately modeled elevator.

The load cases used during the optimizations are listed in Table 2. For the fourth load case the zero fuel weight (ZFW) is used as the analysis weight. For the fifth and sixth load cases the aircraft design weight, W_{des}, is used and computed using the equation: $W_{des} = \sqrt{MTOW(MTOW - W_F)}$.

In this work a wing aerostructural optimization was performed in the presence of the horizontal tail. This means all wing variables

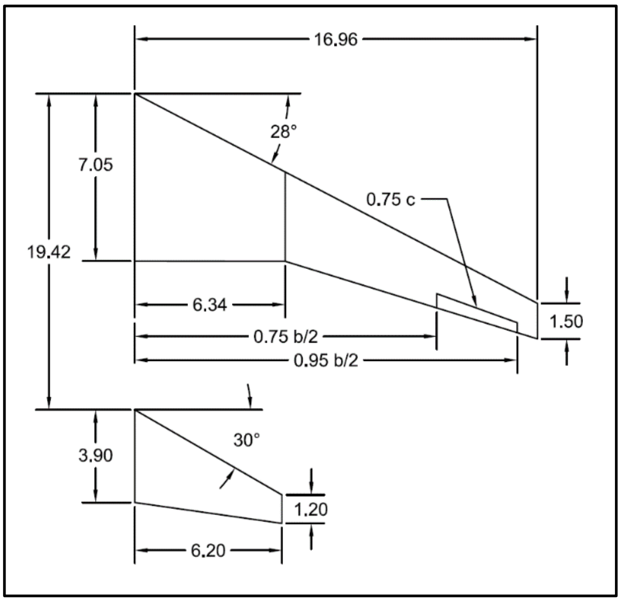

Fig. 2. Planform dimensions (in meters) of A320.

Table 2. Load cases for optimization.

Type	Aircraft weight	Altitude (m)	Mach	Load Factor (g)
pull up	MTOW	7500	0.89	2.5
pull up	MTOW	0	0.58	2.5
push over	MTOW	7500	0.89	-1
gust	ZFW	7500	0.89	1.3
roll	W_{des}	4000	0.83	1
cruise	W_{des}	11000	0.78	1

were included in the design vector and the horizontal was kept constant.

4.2 Aerostructural Optimization

The results of the optimization are shown in the following figures and table. The optimization history plots, including the merit or objective function, feasibility or constraint violation, and optimality are shown in Figure 3. Over the course of the optimization, the normalized objective function was reduced to 0.9183.

Figure 4 shows the change in planform which expectedly shows an increase in span and decrease in sweep, following similar trends as the optimizations conducted in [3]. Table 3 lists key aircraft characteristics from the initial and optimized aircraft. The wing weight was reduced significantly by 12.9% along with the induced drag at 21%. The total drag reduction of 9.6%

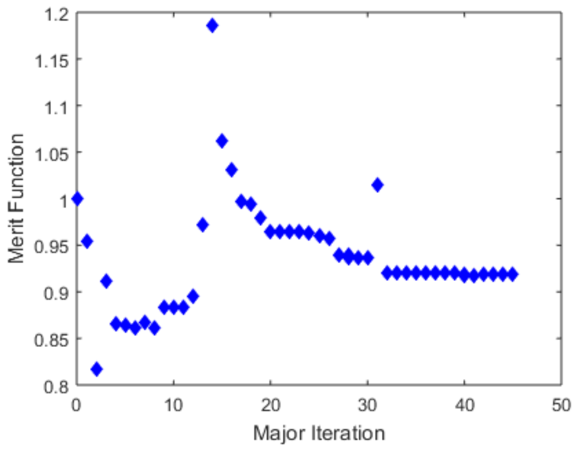

(a)

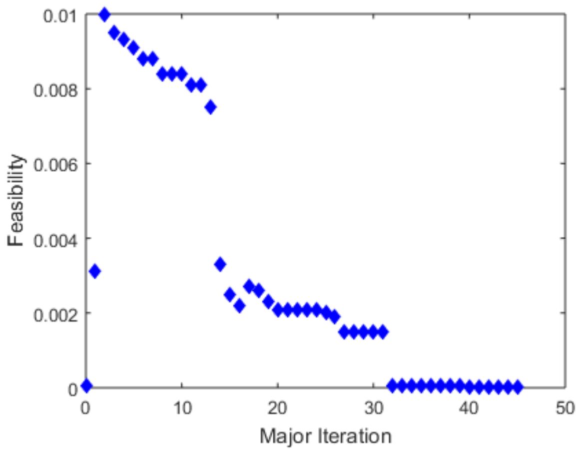

(b)

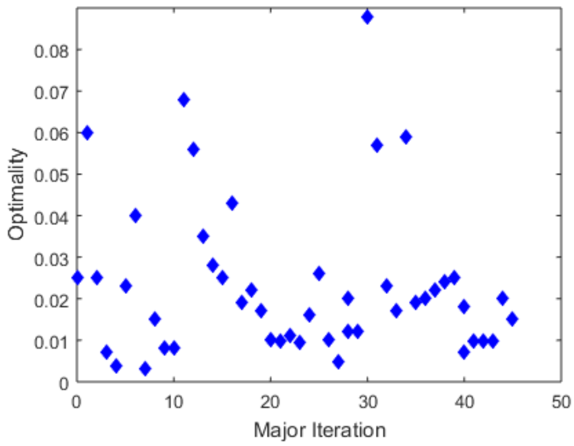

(c)

Fig. 3. Optimization history plots. (a) merit function, (b) feasibility, (c) optimality.

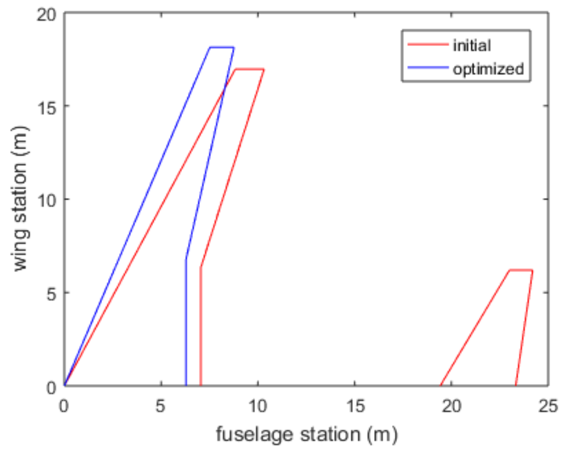

Fig. 4. Initial and optimized planform.

Table 3. Initial and optimized aircraft characteristics.

	Initial	Optimized	Change (%)
Fuel	17940 kg	16477 kg	-8.2
Wing	8861 kg	7719 kg	-12.9
MTOW	73500 kg	70898 kg	-3.5
C_L	0.52	0.53	1.9
C_D	0.0198	0.0179	-9.6
C_{Di}	0.0100	0.0079	-21.0
C_{Df}	0.0063	0.0063	0.0
C_{Dp}	0.0035	0.0037	5.7
S_w	124.2 m^2	119.8 m^2	-3.5

includes a small increase in pressure drag. The horizontal tail weight remained constant, as it was not part of the design vector, however, the failure constraints for the horizontal's panels are still satisfied.

Figures 5 and 6 show the initial and optimized coefficient of pressure, C_p, distributions on selected airfoil sections from the wing span. The initial and optimized airfoil geometries for the respective C_p plots are also shown. Figures 5 and 6 show reductions in the strength of the shock wave along the span, and therefore is likely not the cause for the increase in pressure drag.

Another expected result of the first optimization is due to inadequate stability metrics. The optimized configuration of the aircraft features a lifting tail due to the forward travel of the wing and the fixed center of gravity. In the new configuration the horizontal tail has a lift coefficient of 0.0126, contributing 2.4% of the total lift. Figure 7 shows a C_p plot an airfoil section from the horizontal tail's outer span. In the figure, it is shown that the shock here was in fact strengthened due to the increased load on the tail. This may be the cause of the increase in pressure drag.

While the resulting configuration is optimized and more importantly, the horizontal's failure constraints are satisfied, there are

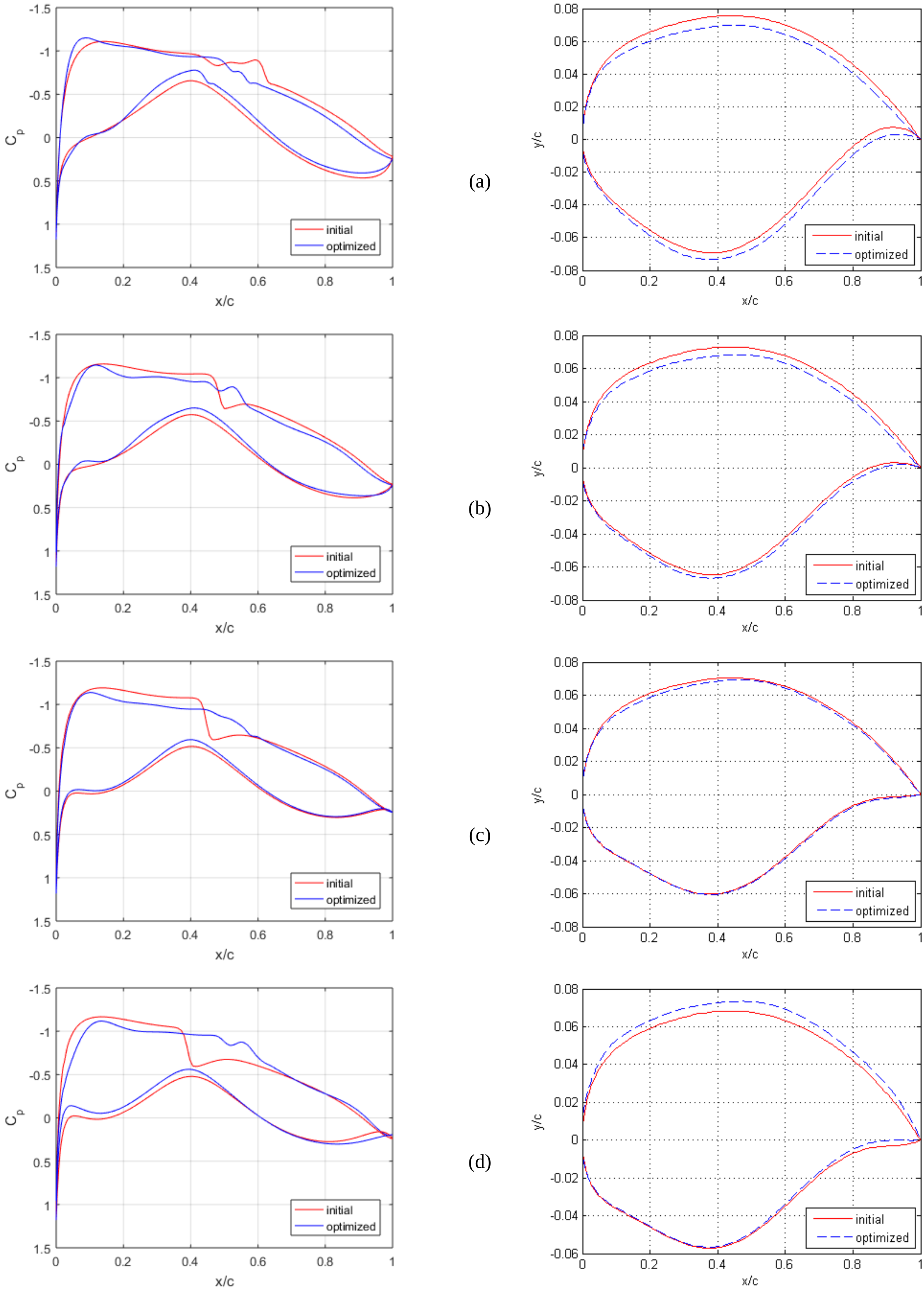

Fig. 5. Initial and optimized coefficient of pressure plots (left) and airfoil geometry (right) at different spanwise positions on wing between 0% and 50% of span length.

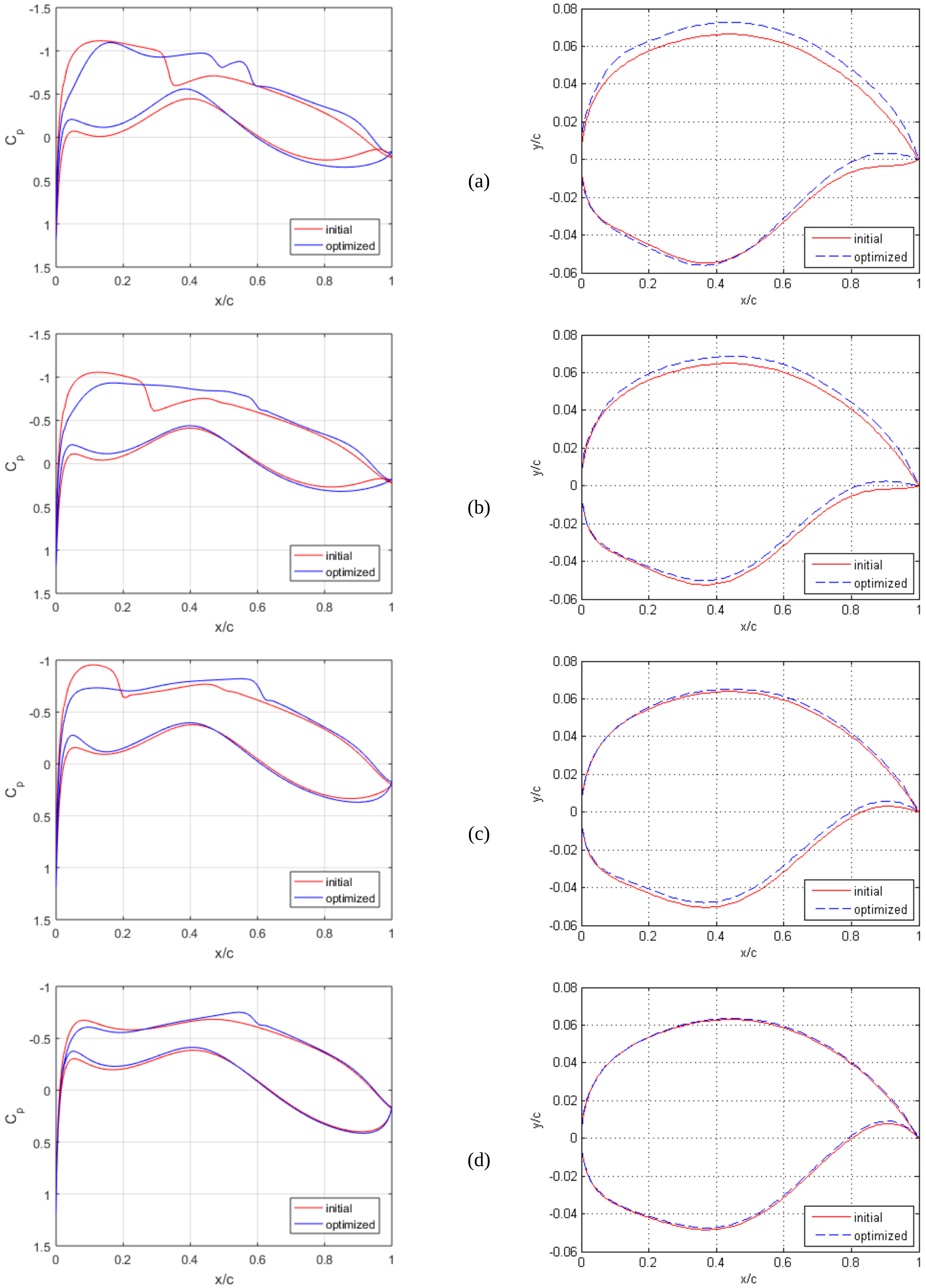

Fig. 6. Initial and optimized coefficient of pressure plots (left) and airfoil geometry (right) at different spanwise positions on wing between 50% and 100% of span length.

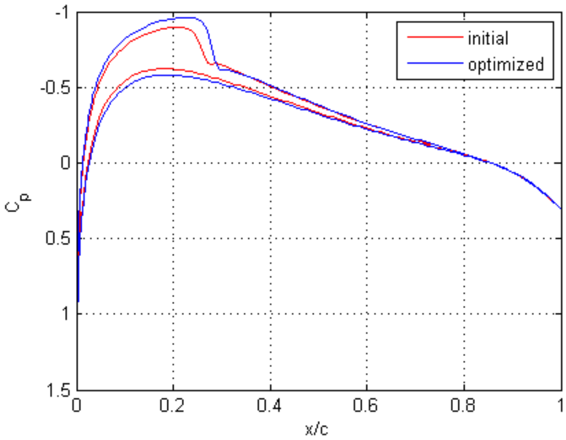

Fig. 7. Coefficient of pressure plot of horizontal stabilizer section from initial and optimized configurations.

currently no stability metrics implemented to insure the horizontal tail performance complies with stability requirements found in the FAA Federal Aviation Regulations (FARs).

5 Conclusions

In this work, aeroelastic and aerostructural optimizations were conducted with a wing and horizontal tail. The aeroelastic optimization sized and validated the wing and horizontal structural weight and the aerostructural optimization successfully optimized all wing design variables while under influence of the horizontal.

The optimizations conducted in this work show that the primary goal, to extend the current design and optimization tool to include the horizontal stabilizer, was achieved. The results also illustrated the importance of considering the full system and the need for additional stability constraints and metrics. With the largest hurdle overcome, additional and essential modules are under development that will improve the weight and center of gravity estimation, making the center a gravity a function of the design vector, as well as implementing the lifting surface pitching moments. This inclusion will increase the drag penalty of the horizontal tail and allow the static margin to be calculated, making full wing and horizontal optimization more feasible and productive.

References

[1] *Flightpath 2050: Europe's Vision for Aviation, Maintaining Global Leadership & Serving Society's Needs, Report of the High Level Group on Aviation Research*. European Union, pp 15, 2011.

[2] Elham A. and van Tooren M. J. L. Beyond Quasi-Analytical Methods for Preliminary Structural Sizing and Weight Estimation of Lifting Surfaces. *56th AIAA/ASCE/AHS/ASC Structures, Structural Dynamics, and Materials Conference*, Kissimmee, Florida, pp 1-19, 2015.

[3] Elham A. and van Tooren M. J. L. Coupled adjoint aeroelastic wing optimization using quasi-three-dimensional aerodynamic analysis. *Structural and Multidisciplinary Optimization*, Vol. 54, No. 4, pp 889-906, 2016.

[4] Katz J and Plotkin A**.** *Low speed aerodynamics*. Cambridge University Press, pp 613, 2001.

[5] Drela M. MSES: Multi-Element Airfoil Design/Analysis Software. Ver. 3.07, Massachusetts Institute of Technology, Cambridge, MA, 2007.

[6] Rump S.M. INTLAB - INTerval LABoratory, *Developments Reliable Computing*, Springer, Dordrecht, pp 77-104, 1999.

[7] Obert E. *Aerodynamic Design of Transport Aircraft.* IOS Press, pp 581, 2009.

[8] Elham A., La Rocca G. and van Tooren M.J.L. Development and implementation of an advanced, design-sensitive method for wing weight estimation. *Aerospace Science and Technology*, Vol. 29, pp 100-113, 2013.

[9] Roskam J. *Airplane Design Part I: Preliminary Sizing of Airplanes*. DARcorporation, Lawrence Kan, 1986.

[10] Martins JRRA. and Lambe A. B. Multidisciplinary Design Optimization: A Survey of Architectures. *AIAA Journal*, Vol. 51, No. 9, pp 2049-2075, 2013.

[11] Gill P., Murray W., and Saunders M. SNOPT: An SQP Algorithm for Large-scale Constrained Optimization. *SIAM*, Vol. 47, No. 1, pp 99-131, 2005.

Contact Author Email Address

a.elham@tu-braunschweig.de

Copyright Statement